Probing decoupled edge states in a zigzag phosphorene nanoribbon via RKKY exchange interaction

SK Firoz Islam,[1,*] Paramita Dutta,[1,†] A. M. Jayannavar,[1,2,‡] and Arijit Saha[1,2,§]
[1]*Institute of Physics, Sachivalaya Marg, Bhubaneswar-751005, India*
[2]*Homi Bhabha National Institute, Training School Complex, Anushakti Nagar, Mumbai 400085, India*

(Received 12 March 2018; published 18 June 2018)

Phosphorene is an anisotropic puckered two-dimensional hexagonal lattice of phosphorus atoms. The edge modes in a zigzag phosphorene nanoribbon are quasiflat in nature and fully isolated from the bulk states, which are unique in comparison to the other hexagonal lattices like graphene, silicene, etc. We theoretically investigate the Ruderman-Kittel-Kasuya-Yosida (RKKY) exchange interaction between two magnetic impurities placed on the nanoribbon and extract the signatures of the flat edge states via the behavior of it. Due to the complete separation of the edge states from the bulk, we can isolate the edge mode contribution via the RKKY interaction from that of the bulk by tuning the external gate potential when both the impurities are placed at the same edge. The bulk-induced RKKY interaction exhibits very smooth oscillation with the distance between the two impurities, whereas for edge modes it fluctuates very rapidly. We also explore the effect of tensile strain both in absence and presence of gate voltage and reveal that the RKKY interaction strength can be boosted under suitable doping, when both the impurities are within the bulk.

DOI: 10.1103/PhysRevB.97.235424

I. INTRODUCTION

In recent times, phosphorene has emerged as a promising 2D material in regards of its potential applications in nanoelectronics owing to the unusual anisotropic band structure [1–3]. It is a bilayer puckered hexagonal lattice of black phosphorus exhibiting both the linear and quadratic energy dispersion in the bulk, depending on the direction of the quasiparticle's momentum. This anisotropy in band structure has recently been exploited in a series of theoretical works, especially in the context of transport properties [4–7]. Apart from the bulk, zigzag phosphorene nanoribbon (ZPNR) can possess two quasiflat edge modes which are completely isolated from the conduction and valence bands [8–12]. This is in complete contrast to the case of other existing 2D hexagonal lattice structures [13–15] where the edge modes merge into the bulk at the two Dirac points. The origin of such a decoupled nature of the flat bands in ZPNR is due to the presence of two out-of plane zigzag chains, coupled by relatively strong hopping parameter, which has recently been addressed by Ezawa [9]. It has also been pointed out that two edge modes can be separated from each other by applying a suitable gate voltage between two opposite transverse edges of the zigzag chain [9]. The 2D phosphorene materials have several advantageous features over the other existing 2D materials, such as phosphorene-based field effect transistor (FET), can be a more suitable device in comparison to a graphene-based FET, especially with regard to switching on/off ratio [3,16,17]. Moreover, charge carriers in phosphorene can acquire very high mobility ($\sim$1000 cm^2/Vs) in comparison to transition metal dichalkogenides materials [3,17,18] ($\sim$200 cm^2/Vs) at room temperature.

The RKKY interaction [19–21] between two magnetic impurities is an indirect exchange interaction mediated by the conduction electrons of the host material. This interaction plays the key role in determining the magnetic ordering in some electronic systems such as spin glasses [22] and alloys [23]. The RKKY interaction has been studied very extensively in various Dirac materials like graphene [24–31], bilayer graphene [32,33], carbon nanotube [34,35], silicene [36,37], topological insulators [38,39], etc. It can be probed by several methods like the single-atomic magnetometry of a pair of magnetic atoms [40,41] and magnetotransport measurement based on angle-resolved photo-emission spectroscopy (ARPES) [42]. Apart from these, a method of directly probing the local spin susceptibility, compatible with 1D nanoribbon, has also been proposed in Ref. [43]. Very recently, the features of RKKY interaction have been proposed to probe the electrically controlled zero energy conducting edge mode in the topological phase of buckled hexagonal silicene lattice structure [37].

Till date, several anisotropic electronic transport properties of phosphorene, as mentioned earlier, have been reported. Nevertheless, the magnetic exchange interaction in presence of magnetic impurities is still under consideration of theoretical investigation as far as phosphorene is concerned. In very recent works, the RKKY exchange interaction has been considered in the bulk of phosphorene, aiming to explore the effect of anisotropy of the band dispersion [44,45]. However, the signatures of unusual quasiflat edge modes in ZPNR have not been explored so far in the context of RKKY interaction, although room temperature magnetism has been explored in detail in Ref. [46]. Apart from the anisotropic nature of the interaction in bulk phosphorene [44,45], the edge modes may play a vital role in the RKKY interaction in ZPNR. Motivated by this, in this paper, we investigate the behavior of RKKY

*firoz@iopb.res.in
†paramitad@iopb.res.in
‡jayan@iopb.res.in
§arijit@iopb.res.in

exchange interaction in ZPNR and extract the responses of quasiflat edge modes from it.

In our work, we consider two magnetic impurities, which are placed either at the same zigzag edge or in the interior of a ZPNR. The features of the quasiflat edge modes in the RKKY interaction are extracted from our numerical results based on the real space Green's function of the system. We observe that the RKKY interaction between two magnetic impurities placed at the same edge of an undoped nanoribbon is much stronger in comparison to the case when any one or both of the impurities are away from the edge. Similar to the other 2D materials, the nature of the interaction is oscillatory with the distance between the two impurities. Moreover, a gate voltage applied between the two nearest zigzag chains, lying at different planes, provides us another degree of freedom to tune the edge modes [11] and, subsequently, RKKY interaction in ZPNR. We show that the strength of the exchange interaction can be significantly enhanced by tuning the gate voltage in undoped ZPNR. It depends on the locations of the impurities as well.

On the other hand, application of strain has significant influences on the band structure as well as topological properties of phosphorene. Very recently, it has been predicted that the application of a tensile or in-plane strain in spin-orbit coupled phosphorene can close and reopen the band gap and gives rise to the topological phase transition [47]. Motivated by this prediction, we also examine the effect of strain on the RKKY interaction both in absence and presence of the gate voltage. However, we do not consider spin-orbit coupling in our ZPNR as, so far, there is no experimental evidence of spin-orbit interaction in monolayer phosphorene. Moreover, we are interested in probing the detached edge modes rather than topological features. The application of a tensile strain can induce a curvature to the band structure for which the RKKY interaction acquires a phase. For all three possible configurations of the location of the impurities i.e., both are at the edge or away from the edge or one at the edge considering the other one within the bulk of the ribbon, we present our results of RKKY interaction to understand the effect of strain. Interestingly, under suitable doping condition, the exchange interaction can be affected by tuning the degree of strain. On the contrary, the combined effect of the gate voltage and strain on the RKKY interaction yields nonsignificant contribution when both the impurities are situated within the interior of the nanoribbon.

The remainder of the paper is organized as follows. In Sec. II, we introduce the lattice structure and the tight-binding Hamiltonian for phosphorene with the inclusion of gate voltage and strain. Section III is devoted to the analysis of band structure of ZPNR under the influence of the gate voltage and strain. A brief discussion on the Green's function formalism for analyzing the RKKY interaction is given in Sec. IV. Our numerical results of the RKKY interaction as a function of the distance between the two magnetic impurities, both in absence and presence of the gate voltages and the tensile strain, are presented in Sec. V. Finally, we summarize and conclude in Sec. VI.

II. TIGHT-BINDING MODEL HAMILTONIAN

In this section, we first provide a short description of the lattice geometry of phosphorene. The puckered hexagonal lattice of phosphorene is very similar to that of graphene but with two nearest-neighbor zigzag chains lying at two different parallel planes. Unlike graphene, the bond lengths as well as corresponding hopping parameters are not identical to each other. It depends on the plane as well as the sublattice of the ribbon. A typical sketch of phosphorene lattice structure is depicted in Fig. 1(a). Also, a top view projected in the x-y plane is shown in Fig. 1(b). Corresponding to the position vector of ith atom r_i, we denote the hopping parameter by t_i. The different structure parameters associated with this lattice structure can be found in Refs. [47,48]. The lattice parameters are given as $r_1 = 22.40\,\text{nm}$, $r_2 = 22.80\,\text{nm}$; $(r_{1x},r_{1y},r_{1z}) = (15.03,16.60,0)\,\text{nm}$, and $(r_{2x},r_{2y},r_{2z}) = (7.86,0,21.40)\,\text{nm}$. Other coordinates r_3,r_4,r_5 can simply be obtained from r_1 and r_2. The two lattice constants in x-y plane are $a = 45.80\,\text{nm}$ and $b = 33.20\,\text{nm}$.

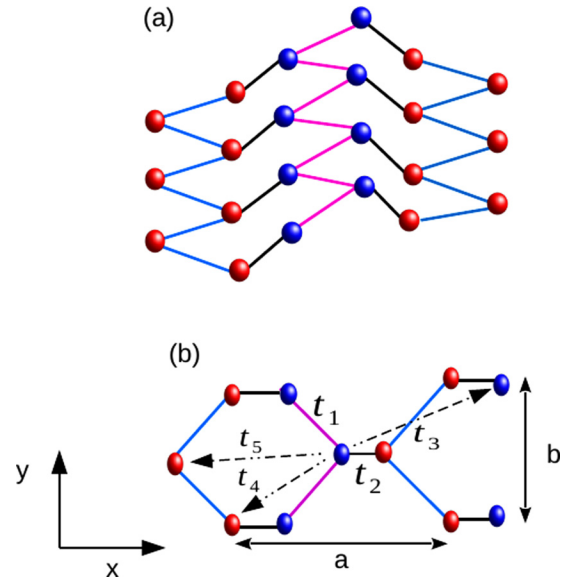

FIG. 1. (a) Schematic view of the phosphorene lattice structure is presented. Two different colors, blue and red, are used to denote the atoms belonging to two different planes. (b) A projected view of the lattice in x-y plane is demonstrated. The five nonequivalent hopping parameters associated with the lattice are marked by t_1, t_2, t_3, t_4, and t_5. a and b are the two lattice constants along the x and y directions, respectively.

The tight-binding Hamiltonian of this puckered lattice, as proposed in Ref. [49], in absence of spin-orbit interaction is given by

$$H_0 = \sum_{ij} t_{ij} c_i^\dagger c_j \,, \tag{1}$$

where the summation in Eq. (1) runs up to the fifth nearest-neighbor and t_{ij} is the hopping parameter between ith and jth atom. The creation (annihilation) operators at ith cite are denoted by $c_i^\dagger$ (c_i). The numerical values of the hopping parameters are [47,49]: $t_1 = -1.22\,\text{eV}$, $t_2 = 3.665\,\text{eV}$, $t_3 = -0.205\,\text{eV}$, $t_4 = -0.105\,\text{eV}$, and $t_5 = -0.055\,\text{eV}$.

A. Inclusion of gate voltage

As the system is composed of two parallel planes of zigzag chain, an application of suitable gate voltage between two opposite edges but in different planes can modify the band structure as pointed out by Ezawa [9] and Ma *et al.* [11] in ZPNR. Note that in-plane hopping parameters are all negative while the interplane hopping parameter (t_2) is positive. However, to tune the full band dispersion with respect to the Fermi level, one can bias the top and bottom planes as $U_t = U$ and $U_b = -U$, respectively. The latter gives rise to an additional band gap $\Delta_g = 2U$. This kind of bias can be realized experimentally [50].

Now, including the effect of the gate voltage, the total Hamiltonian of the system can be written as

$$H = \sum_{ij} t_{ij} c_i^\dagger c_j + \sum_i U c_i^\dagger c_i \,. \tag{2}$$

Here, in our analysis, we bias only the top plane by U and consider the bottom plane at $U = 0$. In the second term of Eq. (2), the index i runs over all the sublattices of the zigzag chain in the top plane only.

B. Inclusion of strain

The strain has a very significant impact on the band structure of 2D sheet of phosphorene. As mentioned previously, phosphorene with spin-orbit coupling can undergo from normal to topological insulator phase transition under suitable in-plane or perpendicular tensile strain [47]. However, in our case, even without spin-orbit coupling, the strain modulates the band structure by modifying the hopping parameters and hence a significant influence on the RKKY magnetic exchange interaction is expected.

When strain is applied, the initial geometrical parameters are deformed as $(r_{ix}, r_{iy}, r_{iz}) = [(1+\epsilon_x)r_{ix}^0, (1+\epsilon_y)r_{iy}^0, (1+\epsilon_z)r_{iz}^0]$, where ϵ_j is the strain along jth direction. In the linear deformation regime, r_i can be simplified up to the first order as

$$r_i = \left(1 + \kappa_x^i \epsilon_x + \kappa_y^i \epsilon_y + \kappa_z^i \epsilon_z\right) r_i^0 \,, \tag{3}$$

with $\kappa_j^i = (r_{ij}/r_i^0)^2$ being the coefficients related to the structural parameters of phosphorene. Finally, following Harrison relation [51], one can obtain the strain-induced modified hopping parameters as

$$t_i \simeq \left(1 - 2\kappa_x^i \epsilon_x - 2\kappa_y^i \epsilon_y - 2\kappa_z^i \epsilon_z\right) t_i^0 \,. \tag{4}$$

However, as it has already been pointed out that the band structure is more sensitive to the perpendicular strain rather than in-plane strain [47], in our analysis we only consider the case $\epsilon_z \neq 0$, while $\epsilon_x = \epsilon_y = 0$.

III. BAND DISPERSION

To find the energy band dispersion of ZPNR (finite along x and infinite along y direction), we write an effective difference equation analogous to the case of an infinite one-dimensional chain [52]. To implement this, the nanoribbon can be considered to consist of an array of the unit cells as shown by the rectangular-shaped, orange-shadowed region in Fig. 2. The

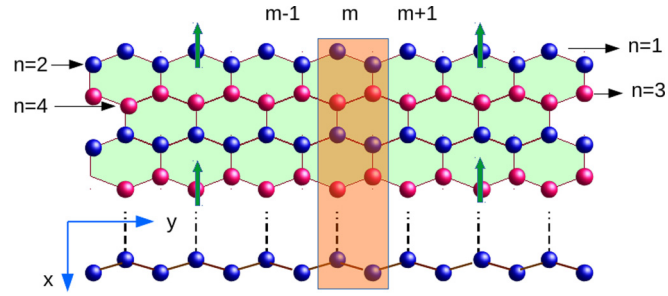

FIG. 2. Schematic of ZPNR with the atoms of two different zigzag chains denoted by two different colors, blue (dark gray) and pink (light gray). The magnetic impurities are denoted by vertical green (light gray) arrow sign. The line numbers along the x and y direction are denoted by the index n and m, respectively.

width of the zigzag ribbon is determined by the number of atoms N per unit cell. The effective difference equation of the ZPNR takes the form as

$$(E\mathcal{I} - \mathcal{E})\psi_m = \mathcal{T}\psi_{m+1} + \mathcal{T}^\dagger \psi_{m-1} \,, \tag{5}$$

where

$$\psi_m = \begin{bmatrix} \psi_{m,1} \\ \psi_{m,2} \\ \vdots \\ \psi_{m,N} \end{bmatrix}, \tag{6}$$

$\mathcal{E}$ and $\mathcal{T}$ are the on-site energy and nearest-neighbor hopping matrices of the unit cells, respectively. $\mathcal{I}$ is the identity matrix of dimension $N \times N$. As the zigzag chain is translationally invariant along y direction, the momentum along that direction (k) is conserved and acts as a good quantum number. Finally, applying Bloch's theorem the total Hamiltonian of the ZPNR can be expressed as

$$(E\mathcal{I} - \mathcal{E}) = \mathcal{T}e^{ikb} + \mathcal{T}^\dagger e^{-ikb} \,, \tag{7}$$

with b as the unit cell separation. The above equation can be solved numerically to yield energy dispersion of the nanoribbon.

In Fig. 3, we show the energy band dispersion of a ZPNR of width $N = 10$ for three different values of gate voltage (a) $U = 0$, (b) $U = 1.5$, and (c) $U = 3$ (in units of t_1). A pair of edge modes (red color), decoupled from the bulk band, appear in the spectra. This is due to the finite width of the ZPNR. We observe that the application of gate voltage causes the shifting of the whole band (consisting of bulk and edge band) by some finite values of energy being proportional to the external gate voltage. Moreover, one of the edge states, which was almost flat in absence of U, is deformed to the curved one for $U \neq 0$. Whereas, in presence of finite U, the shape of the other edge state is changed from concave to convex, maintaining the degenerate or crossing point ($k = \pi$) unchanged.

In Fig. 4, we demonstrate the energy band dispersion of ZPNR under the influence of perpendicular tensile strain. Here, (a), (b), and (c) correspond to different strengths of the strain as $\epsilon_z = 0$, 10%, and 20%, respectively. We note that, unlike the case of the gate voltage, the tensile strain does not manifest any significant shift of the entire band, rather it induces a curvature

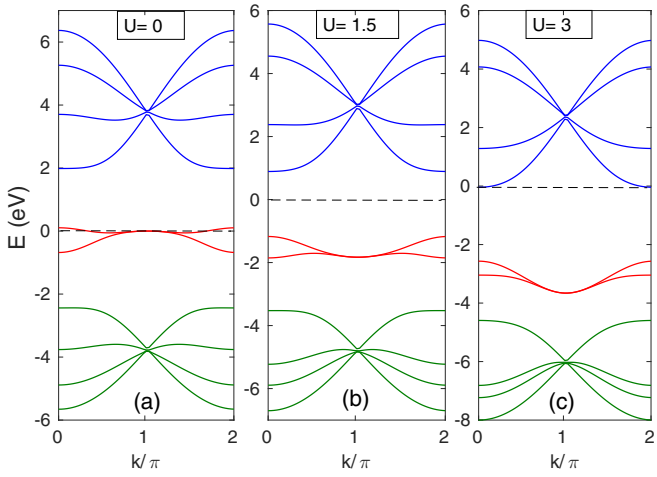

FIG. 3. Energy band dispersion of ZPNR for three different values of gate voltage (in units of t_1) is shown. The width of the ribbon is taken as $N = 10$. The position of the Fermi level is denoted by the dashed line. Here, $\epsilon_z = 0$.

to the bulk modes, leading to the reduction of the band gap. On the other hand, it widens the gap between two edge modes except at $k = \pi$.

Finally, we illustrate the band dispersion of ZPNR in presence of both gate voltage and strain in Fig. 5. Here, we consider the gate voltage to be fixed at $U = 3t_1$ and vary the strain as $\epsilon_z = 0$, 10%, and 20% in (a), (b), and (c), respectively. However, in this case, the band dispersion appears to be less sensitive to the strain compared to the case in Fig. 4. The issue of band gap reduction or band curvature of the bulk states seems to be insensitive to the combined effects of strain and gate voltage. However, the edge modes still preserve the curvature under the influence of the strain even in presence of the gate voltage. Additionally, the interband separation within the bulk

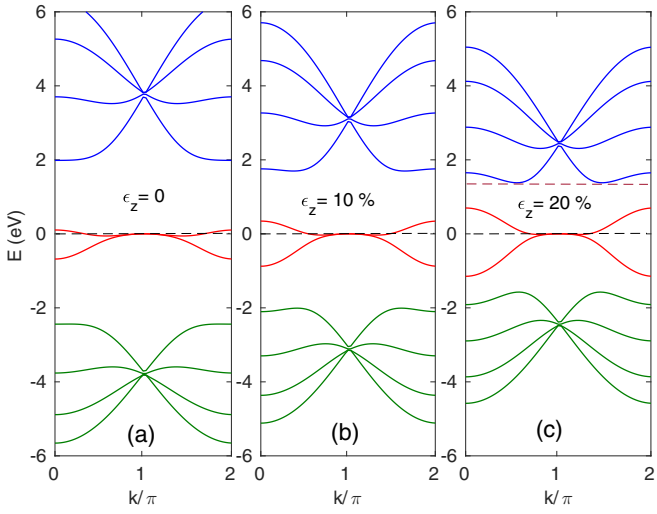

FIG. 4. The features of energy band dispersion of ZPNR for three different strengths of tensile strain is illustrated when $U = 0$. The width of the ribbon is considered to be the same as mentioned in Fig. 3. Two different positions of the Fermi level are denoted by a dashed line.

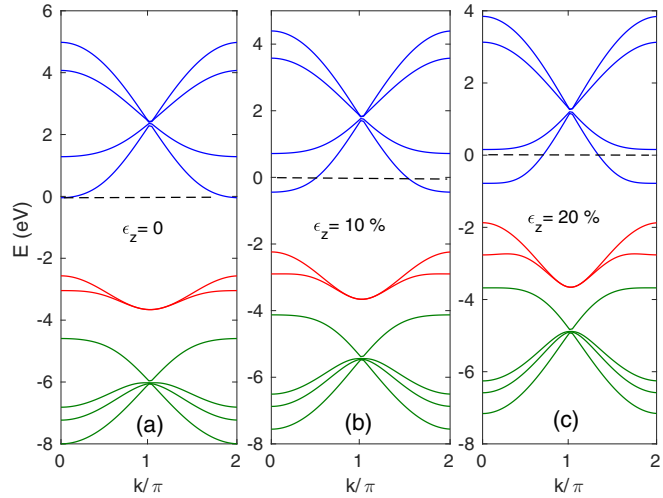

FIG. 5. Energy band dispersion of ZPNR is illustrated for three different strengths of tensile strain in presence of a fixed nonzero gate voltage $U = 3t_1$. The width of the ribbon is the same as mentioned in Fig. 3. The position of the Fermi level is marked by the dashed line.

band changes with the enhancement of strain for a finite gate voltage.

IV. THEORETICAL FORMALISM OF RKKY INTERACTION

In our analysis, we consider the two magnetic impurities located at (m_1,n_1) and (m_2,n_2) sites (following the notations of Fig. 2) of the nanoribbon. The indirect exchange interaction between these two magnetic impurities is mediated by the conduction electrons of the host material. The Hamiltonian for the exchange interaction between the spin of the magnetic impurity (S) and the conduction electron (s) can be written as

$$H_{\rm int} = J_c \sum_{\alpha} S_\alpha . s_\alpha \ , \tag{8}$$

where α is the sublattice index. By implementing the well-known RKKY perturbation theory, the exchange interaction energy between the spins of two magnetic impurities can be expressed in terms of the Heisenberg form as [19–21,29,37]

$$E(\mathbf{r}) = J_{\alpha\beta}(\mathbf{r}) S_\alpha . S_\beta \ . \tag{9}$$

Here, one of the two impurities is located at the origin and the other one at position $\mathbf{r}$. Here, α and β represent the sublattice index on which magnetic impurities are placed and $J_{\alpha\beta}$ is the strength of the exchange coupling between the two impurities which is linked to the spin-independent susceptibility $\chi_{\alpha\beta}$ as

$$J_{\alpha\beta} = C \chi_{\alpha\beta} \ , \tag{10}$$

where $C = (J_c\hbar/2)^2$. The static susceptibility can be evaluated from the retarded Green's function as

$$\chi_{\alpha\beta}(\mathbf{r},\mathbf{r}') = -\frac{2}{\pi} {\rm Im} \int_{-\infty}^{E_F} dE \big[G^0_{\alpha\beta}(\mathbf{r},\mathbf{r}',E) G^0_{\alpha\beta}(\mathbf{r}',\mathbf{r},E) \big]. \tag{11}$$

Here, $G^0_{\alpha\beta}$ is the spin-independent unperturbed single particle Green's function, which can be expressed in the spectral

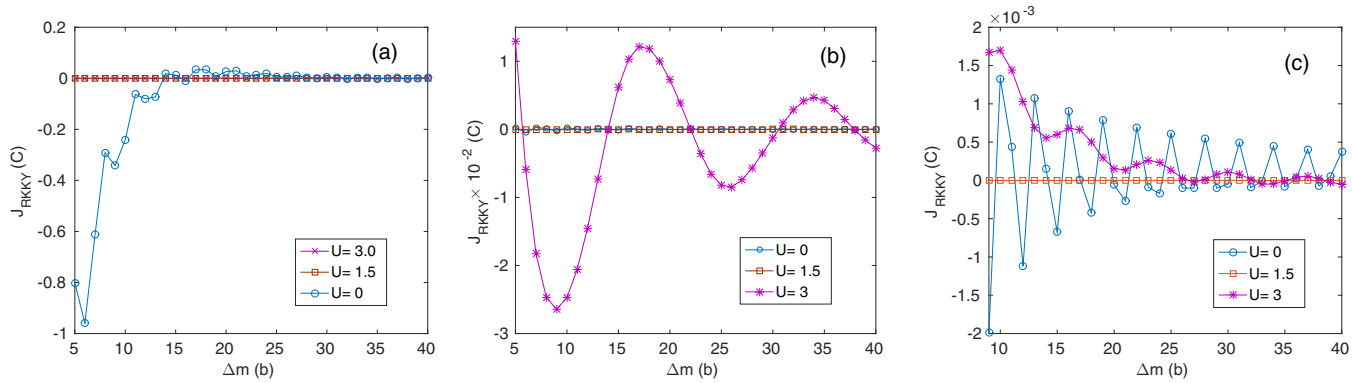

FIG. 6. The behavior of RKKY exchange interaction (in units of $C = (J_c\hbar/2)^2$) between two magnetic impurities is demonstrated as a function of the distance (in units of the lattice parameter b) between them when (a) both the impurities are at the same edge, (b) both are within the bulk of ZPNR, and (c) one at the edge, while the other one is located in the interior of the ZPNR. The size of the undoped ribbon is 10×100. For each case, three different gate voltages, $U = 0$, 1.5, and 3 (in units of t_1) are considered. Here, we choose the strain $\epsilon_z = 0$.

representation as

$$G^0_{\alpha\beta}(\mathbf{r},\mathbf{r}',E) = \sum_n \frac{\psi^\alpha_n(\mathbf{r})\psi^\beta_n(\mathbf{r}')}{E - E_n + i\eta}, \tag{12}$$

where n runs over all the eigenstates which has to be evaluated by diagonalizing Eq. (2) for a finite size lattice.

V. NUMERICAL RESULTS AND DISCUSSION

In this section, we present our numerical results of the RKKY interaction ($J_{\rm RKKY}$), in units of C, between the two magnetic impurities for various combinations of their locations in ZPNR. We consider three different situations when both the impurities are located at the same edge of the nanoribbon, or they are situated within the bulk, or one impurity is located at the edge, while the other one is situated in the interior of the ribbon. We discuss the effect of gate voltage, tensile strain, and their combination in three different subsections. The size of the ZPNR is considered as the length $M = 100$ and width $N = 10$. Note that any further increase of the length of the ZPNR will not alter the qualitative nature of our main results. Similarly, the higher value of N does not modulate the RKKY interaction significantly for the undoped situation. The reason can be attributed to the fact that, if we enhance the width of the ribbon, the number of bulk modes increases without affecting the edge states. On the other hand, the RKKY interaction for the undoped condition is strongly dependent on the behavior of the edge modes. Hence, even for wider ribbon, our results will change quantitatively while the qualitative features will remain unaffected.

A. Effect of external gate voltage

In Fig. 6, we present our results for the RKKY exchange interaction between two magnetic impurities for an undoped ($E_F = 0$) ZPNR, as a function of the distance between them. We employ Eq. (10) to compute the RKKY exchange interaction. We choose three different impurity configurations within the lattice as mentioned earlier. Here, Fig. 6(a) corresponds to the case when both the impurities are placed at the same edge. We fix one of the impurities at the position $(1,m_1)$ and the location of the second impurity is at $(1,m_2)$. In our numerical analysis, we vary Δm $(= m_2 - m_1)$ from 5 to 40 (in units of the lattice parameter b). We observe that the behavior of $J_{\rm RKKY}$ with Δm is oscillatory in nature. This oscillatory behavior with distance between the impurities comes out to be very similar to that of other 2D Dirac materials as reported earlier in the literature [29,37,39]. The amplitude of the oscillation decays very fast as we increase the distances between the two impurities. However, for the case of nanoribbon where we deal with the lattice model instead of continuum as in the bulk, exact functional dependence is difficult to establish. Nevertheless, from our numerical analysis, we can only predict that the pattern of the RKKY interaction exhibits close resemblance to $1/R^3$ decay. The characteristic feature of RKKY interaction in ZPNR, in absence of gate voltage, is very similar to that of graphene, as discussed in Ref. [29]. To discuss the effect of external gate potential, we choose three different values of U $(= 0,$ 1.5, and 3 in units of $t_1)$. We observe that $J_{\rm RKKY}$ attains maximum strength when the applied gate voltage is zero. The RKKY interaction becomes vanishingly small with the increase of the gate voltage U [see Fig. 6(a)]. The reason behind this phenomenon can be explained from the features of band structure as shown in Fig. 3. For $U = 0$, the Fermi level crosses the decoupled edge states. As soon as we switch on the gate voltage, the Fermi level moves away from the edge modes to the gap between the bulk and edge states where the density of states are vanishingly small to conduct. As the bands near the Fermi levels contribute to tunneling exchange, the RKKY interaction strength becomes vanishingly small due to the unavailability of the DOS for $U \neq 0$. On the other hand, the origin of the RKKY interaction can be purely attributed to the edge states of the ZPNR when $U = 0$. The contribution of the bulk states are almost zero as both the impurities are located at the edge of the ribbon. Hence, one can separately probe the edge states of ZPNR via the RKKY interaction. These features of the RKKY interaction can be further analyzed in terms of local density of states (LDOS) expressed for ith site as

$$\rho_i = -\frac{1}{\pi}\mathrm{Im}[G_{ii}(\mathbf{r},\mathbf{r},E)]. \tag{13}$$

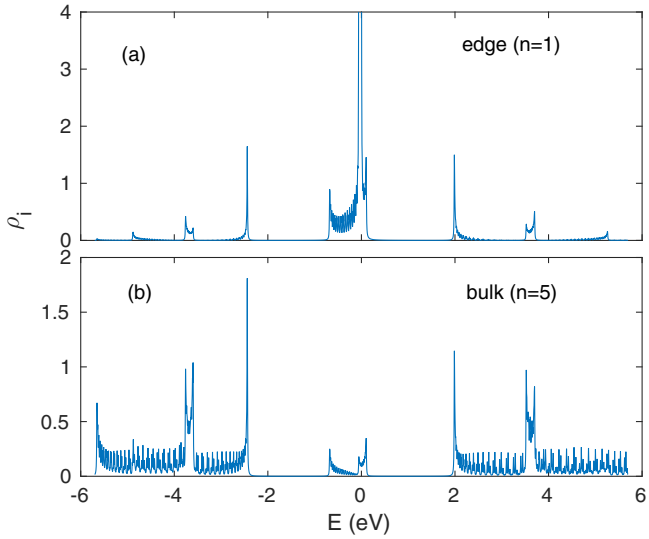

FIG. 7. The behavior of LDOS is shown as a function of energy for (a) edge states ($n = 1$) and (b) bulk states ($n = 5$). Here, we have considered $m = 26^{th}$ unitcell.

The LDOS is demonstrated in Fig. 7, which manifests the existence of relatively higher LDOS around the zero energy corresponding to edge states ($n = 1$) in comparison to the bulk ($n = 5$). The other peaks in LDOS around $E = +2$ eV and -2.2 eV, present in both Figs. 7(a) and 7(b), correspond to the bulk states. The asymmetry around zero energy corroborates the particle-hole asymmetry in the band structure described above. Also, this asymmetry has been reported earlier in the context of band structure [7]. The central peak is well separated from the bulk for which the RKKY interaction becomes vanishingly small when the Fermi level is tuned into the gap between the central and nearest bulk peaks.

Here, we present a comparative analysis between ZPNR and other hexagonal lattices like graphene and silicene in the context of RKKY interaction. The graphene zigzag nanoribbon also consists of zero energy edge modes as well as gapless bulk states, which are in contrast to ZPNR where the bulk is gapped. Apart from that, the edge modes are not isolated from the bulk states. Rather, they merge into the bulk at the two valleys [13], for which a small deviation from the undoped case would not cause any sudden drop in the RKKY interaction as the Fermi level always passes through the edge modes. Moreover, as the bulk is gapless, the contribution of edge states on the RKKY interaction in an undoped graphene zigzag nanoribbon will always be accompanied by the bulk states. In case of silicene [14], although it exhibits gapped bulk band structure due to the strong spin-orbit interaction owing to buckled lattice structure, the edge modes are not decoupled from the bulk. Whereas, the edge modes in ZPNR are fully separated from the bulk, which yields a sudden drop in the RKKY interaction amplitude after a small deviation of the Fermi level from the edge modes by means of a gate voltage. This unique nature of the edge states in ZPNR allows one to probe them separately from the bulk.

In Fig. 6(b), we consider the case when both the impurities are away from the edge. The locations of the two magnetic impurities are considered at $(5,m_1)$ and $(5,m_2)$. We vary Δm from 5 to 40 (in units of b) as mentioned in the previous case. We observe that the RKKY interaction is negligibly small even as the Fermi level passes through the decoupled edge states as shown in Fig. 3. As the Fermi level is far away from the bulk states, it leads to vanishingly small contribution to the exchange interaction in undoped situations when both the impurities are situated in the interior region of the ZPNR. The DOS due to the edge modes doesn't contribute to RKKY for $U = 0$. By the application of gate voltage, the energy band dispersion inside the bulk as well as the edge modes are shifted and the bulk states come closer to the Fermi level for which RKKY interaction inside the bulk becomes significant. At gate voltage $U = 3t_1$, the RKKY interaction manifests smooth oscillation with relatively higher amplitude [see Fig. 6(b)]. Such higher amplitude is the consequence of the availibility of large DOS due to the bulk bands as the Fermi level crosses them (see Fig. 3). Hence, a clear distinction between the nature of the RKKY exchange interactions for bulk and edge modes are now visible. The strength of RKKY interaction displays a smooth oscillation with higher amplitude when both the impurities are located within the bulk whereas; it oscillates rapidly and decays very fast in the case when we place them at the edge of the ZPNR.

Finally, we consider the case when one magnetic impurity is situated at the edge and the other one is located within the bulk. The locations of the two impurities are at $(1,m_1)$ and $(5,m_2)$ and Δm is varied as mentioned before. The corresponding behavior of RKKY interaction, for this situation, is illustrated in Fig. 6(c). Here, we observe that the RKKY interaction is dominated by the edge modes when $U = 0$. However, with the further enhancement of the gate voltage ($U \neq 0$), the bulk states also start to contribute, for which a smooth oscillation with higher frequency appears in the behavior of RKKY. This oscillation is mostly confined within the regime of positive (ferromagnetic) sign of the interaction [see Fig. 6(c) and $U = 3t_1$ in particular].

Therefore, in all the above three cases, depending on the gate voltage, the interplay of the Fermi level and the LDOS (edge/bulk) gives rise to the desirable RKKY exchange interaction between the two magnetic impurities. However, the features of exchange interactions still differ from each other in terms of nature of oscillation.

At this stage, we also show how the RKKY interaction behaves with the variation of the gate voltage in Fig. 8 for fixed distance between the two impurities located at the same edge. We observe that when the gate voltage is zero, the RKKY interaction is maximum and it decays very fast associated by small fluctuation with the enhancement of gate voltage. Such sharp reduction in amplitude with respect to the gate voltage is expected as the Fermi level deviates from the decoupled edge states for large U. This small contribution with fluctuation even for a finite gate voltage is the consequence of small density of states around the edge modes. Note that the behavior of the RKKY interaction for different values of $\Delta m(= 12, 14)$ is almost similar as far as amplitude and phase mismatch are concerned. This is expected as we have already demonstrated previously that the RKKY interaction exhibits rapid fluctuation with the distance between the two magnetic impurities [see Fig. 6(a)].

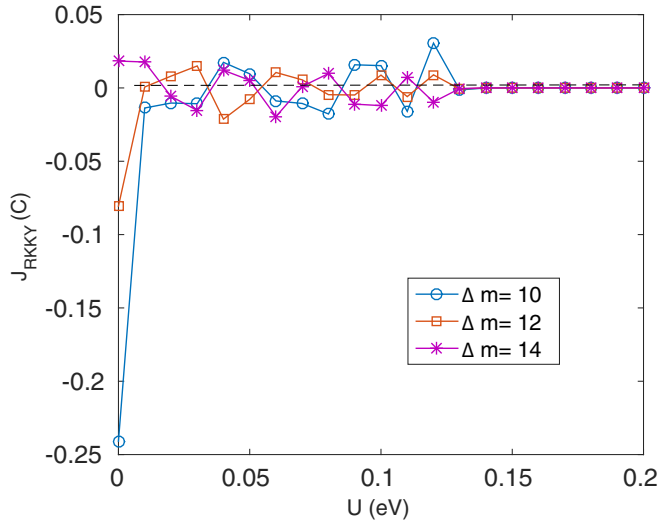

FIG. 8. The feature of RKKY interaction strength (in units of C) is illustrated with respect to the gate voltage for three different spatial distributions (in units of b) of two magnetic impurities.

B. Effect of tensile strain

In this subsection, we investigate how the strength of RKKY interaction responds to the different degrees of tensile strain. Considering the same system size, RKKY interaction strength is numerically computed for various spatial configurations of the two magnetic impurities as mentioned in Fig. 6.

In Fig. 9(a), we show the behavior of J_{RKKY} as a function of Δm for an undoped ZPNR, considering the case when both the magnetic impurities are at the same edge. We observe that for small separation between the two impurities, the RKKY interaction is strong with only negative sign (antiferromagnetic). However, it decays exponentially fast and becomes vanishingly small as we increase the distance between them. Moreover, the RKKY interaction seems to be very weakly sensitive to the degree of strain in this case. This can be explained by the band structure analysis of the undoped strained ZPNR (see Fig. 4). As the Fermi level crosses through the edge states, irrespective of the degree of strain, the amplitude of the RKKY interaction remains almost unaffected with the strain. Although the bulk states of the ribbon get affected by the applied strain, it does not reflect in the feature of RKKY interaction as both the impurities are located at the edge of the ribbon.

Similar to the case of gate voltage, we also consider the situation where both the impurities are located in the interior of the undoped nanoribbon. Our corresponding results for the RKKY interaction as a function of Δm are depicted in Fig. 9(b). The strength of the interaction abruptly falls down in this case compared to the earlier case where the impurities were situated at the edge. This occurs as the bulk states are away from the Fermi level of the undoped ribbon as shown in Fig. 4. Hence, the available DOS to mediate RKKY interaction in this case is vanishingly small. Therefore, although the impurity positions are within the bulk region, the amplitude of the RKKY interaction is still relatively small as only the edge states being close to the Fermi level can mediate the exchange interaction. The variation of the degree of strain also does not affect the strength of the interaction significantly—even the bulk states are deformed substantially with strain. The reason is that the bulk states are well separated from the Fermi level by a substantial gap even with $\epsilon_z = 20\%$. However, the enhancement of strain induces a small phase to the oscillation of the RKKY interaction. Note that as far as the oscillatory nature of the interaction in concerned, switching the phase from ferromagnetic to the antiferromagnetic order and vice versa is still present. This feature is very similar to the other 2D materials [29,37].

In Fig. 9(c), we demonstrate the behavior of RKKY interaction for the case when one impurity is at the edge and the other one is inside the bulk of the undoped ZPNR. This also manifests oscillatory behavior with distance between the two impurities. Such oscillatory nature as well as the amplitude of the interaction are almost insensitive to the strain. However, the strength of the interaction increases in comparison to the case shown in Fig. 9(b). This happens as one of the impurities is located at the edge of the ribbon and the available DOS due to the edge states contributes to the finite value of J_{RKKY}.

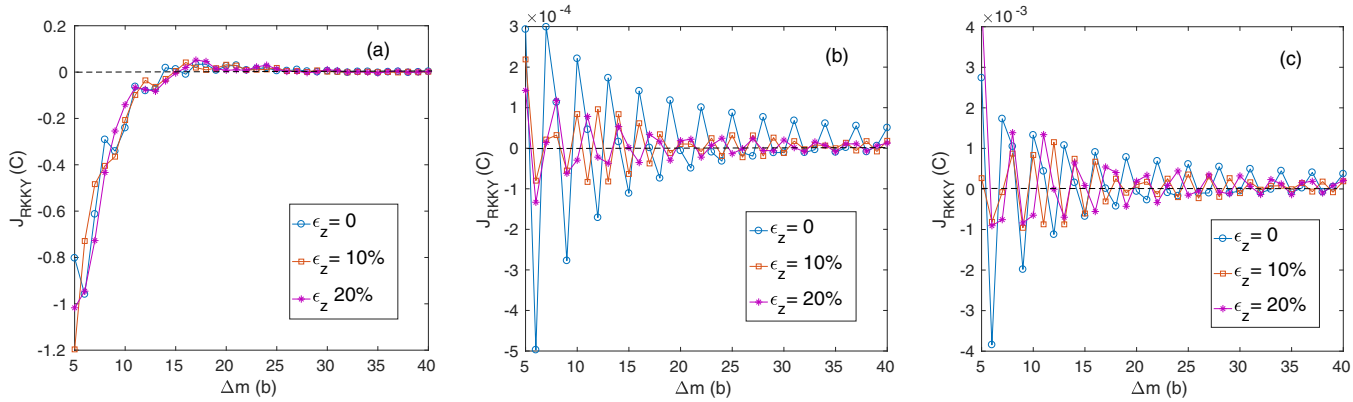

FIG. 9. The behavior of RKKY exchange interaction (in units of $C = (J_c\hbar/2)^2$) between two magnetic impurities is illustrated as a function of the distance (in units of lattice parameter b) between them when (a) both the impurities are at the same edge, (b) both are within the bulk, and (c) one at the edge while the other one within the bulk. The size of the undoped ($E_F = 0$) ZPNR is 10×100. For each case, three different values of strain, $\epsilon_z = 0$, 10% and 20% (in units of t_1) are taken into account in absence of any gate voltage ($U = 0$).

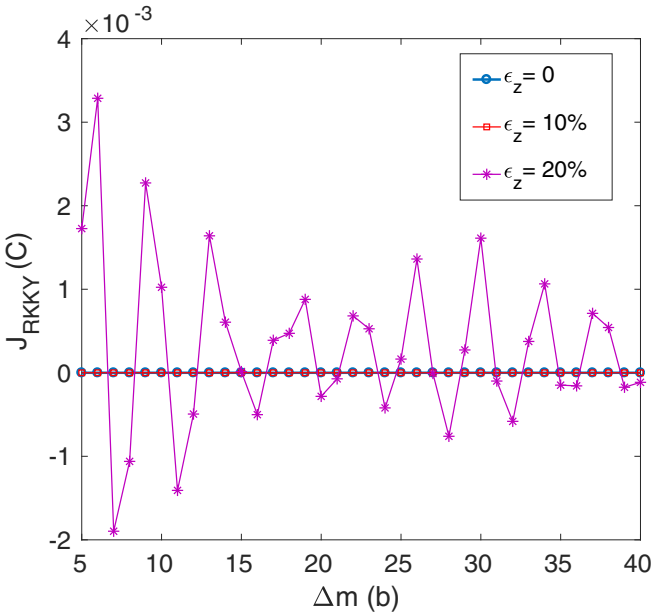

FIG. 10. The behavior of RKKY interaction strength (in units of C) between two impurities is illustrated as a function of distance (in units of b) between them when both the impurities are inside the bulk. The ZPNR is doped at $E_F = 1.6t_1$ and $U = 0$. We choose the same size of the ribbon as mentioned in Fig. 9.

So far, we have considered undoped ribbon ($E_F = 0$). From the band structure shown in Fig. 4, we can conclude that the RKKY interaction strength may enhance significantly if one dopes the system locating both the impurities within the bulk region of the ZPNR. We illustrate the behavior of J_{RKKY} as a function of the relative separation between the impurities in Fig. 10. We choose three different values of the strain (0, 10%, and 20%), after tuning the Fermi level at $E_F = 1.6$ (in units of t_1). We observe that the RKKY interaction strength in the doped ZPNR increases significantly when we apply high degree of strain. For example, the exchange interaction becomes very strong for the strain of 20% in comparison to zero and 10%. The reason can be attributed to the band dispersion (see Fig. 4) which exhibits that Fermi level lies far away from the bulk states when strain is considered to be at zero and 10%. However, as we apply strong degree of strain (20%), then it induces a strong curvature to the bulk bands and effectively reduces the band gap between the bulk states. Thus, the Fermi level intersects the bulk bands. This induces a sizable contribution to the RKKY interaction between the two magnetic impurities positioned inside the bulk region of the doped ZPNR. Note that RKKY exchange interaction also exhibits a beating pattern around $\Delta m = 20$. This appears due to the superposition of two contributions arising from the two closely spaced different momenta, as the Fermi level passes through them [see Fig. 4(c) for illustration].

C. Combined effect of gate voltage and strain

Here, we consider the case when both the gate voltage and the strain are applied together to the undoped ($E_F = 0$) ZPNR. We present our results of the RKKY exchange interaction as a function of the spatial separation between the impurities in

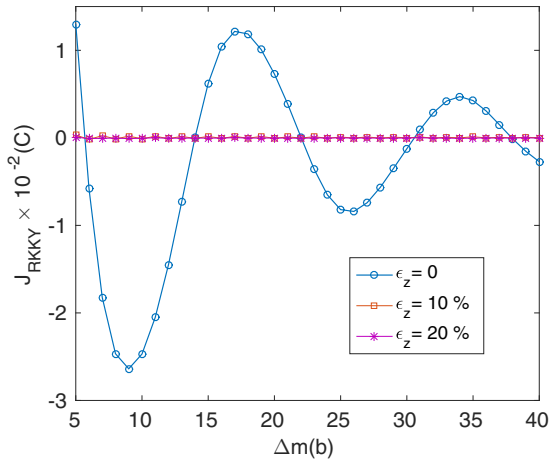

FIG. 11. The feature of RKKY exchange interaction (in units of C) between two magnetic impurities, located inside the bulk of a ZPNR, is demonstrated as a function of the distance (in units of b) between them. We choose $U = 3t_1$, $E_F = 0$ and the same size of the ribbon as mentioned in Fig. 9.

Fig. 11, for three different values of the strain. We also consider nonzero gate voltage at $U = 3t_1$ for which the Fermi level lies very close to the bulk band and far away from the edge modes (see Fig. 5). Therefore, this configuration gives rise to the dominant contribution in the RKKY exchange only when both the impurities are inside the bulk. Also, the exchange interaction becomes vanishingly small when one of the two impurities or both the impurities reside at the same edge due to the unavailability of sufficient DOS to mediate RKKY. Furthermore, in this case, we observe a smooth oscillation in the behavior of J_{RKKY} for $\epsilon_z = 0$, which is already discussed in the earlier subsection in the context of gate voltage [see Fig. 6(b)]. However, with the enhancement of strain, the RKKY

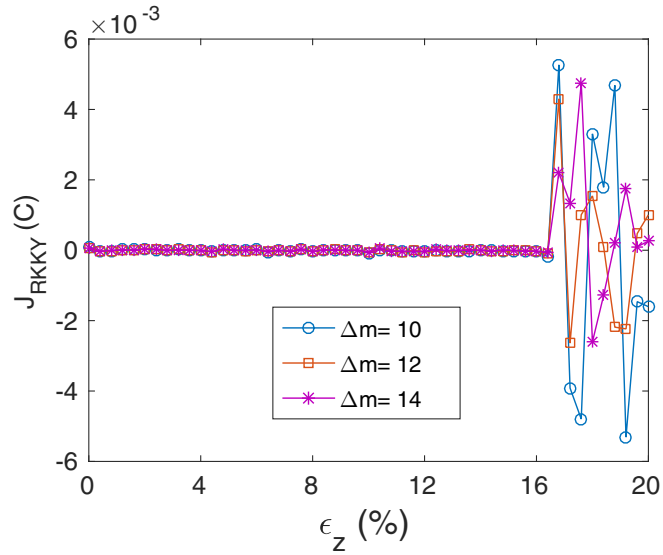

FIG. 12. The behavior of RKKY interaction strength (in units of C) is illustrated as a function of degree of strain for three different spatial distributions (in units of b) of two impurities. We consider finite doping $E_F = -2$ eV and gate voltage $U = 3$ eV.

interaction suddenly drops to zero. The reason can be attributed to the fact that, as we increase the degree of strain, the band gap between the conduction and valence band reduces, and subsequently the Fermi level is repositioned much inside the bulk states. The strength of the RKKY interaction is inversely proportional to the Fermi momentum. This causes sudden drops in exchange interaction strength when we tune the strain to 10% or 20%. The corresponding band dispersion in presence of both gate voltage and strain, depicted in Fig. 5, manifests that Fermi level E_F intersects the bulk bands with higher momentum for higher degree of strain and, consequently, it weakens the exchange interaction mediated through the conduction electrons.

Similar to the plot of RKKY interaction with respect to gate voltage shown in Fig. 8, we here depict the behavior of RKKY interaction strength with the variation of strain in Fig. 12. We choose three different values of Δm and a particular value of gate voltage U. To obtain better signatures of strain on the RKKY interaction, we have chosen ZPNR with finite doping. The corresponding band dispersion for that case is shown in Fig. 5. The RKKY interaction remains vanishingly small till the degree of strain reaches $\epsilon_z = 16\%$ when the edge modes start overlapping with the Fermi level. Beyond this degree of strain, the RKKY interaction shows sudden rise with large fluctuations. A general statement regarding such behavior of the amplitude of the RKKY interaction can be attributed to the interplay of Fermi level with the band dispersion (edge modes or bulk states).

VI. SUMMARY AND CONCLUSIONS

To summarize, in this paper, we numerically investigate the RKKY exchange interaction between two magnetic impurities located on a zigzag phosphorene nanoribbon. The signatures of quasiflat edge modes via RKKY interaction in ZPNR have been explored. We show that the small deviation of the Fermi level, by means of gate voltage, gives rise to a sudden drop in the strength of the RKKY interaction between the two magnetic impurities positioned at the same edge. Note that this sudden drop is a consequence of the separation between the edge and the bulk states and LDOS therein. When the Fermi level lies within the gap between the edge and bulk states, the density of states of the conduction electrons is negligibly small to contribute significantly to the RKKY exchange phenomenon. On the other hand, in other 2D Dirac materials like graphene and silicene zigzag nanoribbon, we cannot separately identify the contributions of the edge states as they merge inside the bulk bands. In undoped graphene, the contribution of edge modes to the RKKY interaction is always accompanied by the bulk contribution i.e., they are inseparable. Whereas in silicene, although it possesses a band gap due to the spin-orbit interaction, the edge modes are not fully decoupled from the bulk and merge inside the bulk bands at two valleys. Hence, one cannot separate out their contributions to the RKKY interaction too. Therefore, phosphorene is a semi-Dirac material in which the separation of quasiflat edge modes and the isolation of its contribution via the RKKY exchange interaction can be a possible probe to detect them in a ribbon geometry. Moreover, the nature of the oscillations in the RKKY interaction are in complete contrast to each other in ZPNR, when both the impurities are in the bulk or at the same edge. We also consider the effect of tensile strain on RKKY exchange interaction. The strain does not impart any shift to the band dispersion, rather it attributes a curvature to the bulk bands. Such curvature introduces an additional phase shift to the RKKY oscillation with the distance between the two impurities. The amplitude of the exchange interaction is weakly sensitive to the strain value. However, one can enhance the strength of the interaction by adjusting the Fermi level at suitable position. Finally, we also explore the case when both gate voltage and strain are applied simultaneously to the ZPNR. In this case, the amplitude as well as the oscillation of the interaction profile is very sensitive to the Fermi energy too.

ACKNOWLEDGMENTS

P.D. thanks Department of Science and Technology (DST), India, for the financial support through SERB NPDF (File No. PDF/2016/001178). A.M.J. also thanks DST, India, for financial support through a J.C. Bose Fellowship.

[1] H. Liu, A. T. Neal, Z. Zhu, Z. Luo, X. Xu, D. Tománek, and P. D. Ye, ACS Nano **8**, 4033 (2014).
[2] A. Castellanos-Gomez, Nat. Photonics **10**, 202 (2016).
[3] S. P. Koenig, R. A. Doganov, H. Schmidt, A. Castro Neto, and B. Özyilmaz, Appl. Phys. Lett. **104**, 103106 (2014).
[4] B. Ghosh, P. Kumar, A. Thakur, Y. S. Chauhan, S. Bhowmick, and A. Agarwal, Phys. Rev. B **96**, 035422 (2017).
[5] X. Wang, A. M. Jones, K. L. Seyler, V. Tran, Y. Jia, H. Zhao, H. Wang, L. Yang, X. Xu, and F. Xia, Nat. Nanotechnol. **10**, 517 (2015).
[6] J. Linder and T. Yokoyama, Phys. Rev. B **95**, 144515 (2017).
[7] M. Zare, B. Z. Rameshti, F. G. Ghamsari, and R. Asgari, Phys. Rev. B **95**, 045422 (2017).
[8] A. Maity, A. Singh, P. Sen, A. Kibey, A. Kshirsagar, and D. G. Kanhere, Phys. Rev. B **94**, 075422 (2016).
[9] M. Ezawa, New J. Phys. **16**, 115004 (2014).
[10] E. Taghizadeh Sisakht, M. H. Zare, and F. Fazileh, Phys. Rev. B **91**, 085409 (2015).
[11] R. Ma, H. Geng, W. Y. Deng, M. N. Chen, L. Sheng, and D. Y. Xing, Phys. Rev. B **94**, 125410 (2016).
[12] B. Ostahie and A. Aldea, Phys. Rev. B **93**, 075408 (2016).
[13] A. H. Castro Neto, F. Guinea, N. M. R. Peres, K. S. Novoselov, and A. K. Geim, Rev. Mod. Phys. **81**, 109 (2009).
[14] K. Shakouri, H. Simchi, M. Esmaeilzadeh, H. Mazidabadi, and F. M. Peeters, Phys. Rev. B **92**, 035413 (2015).
[15] SK Firoz Islam and P. Dutta, Phys. Rev. B **96**, 045418 (2017).
[16] S. Das, M. Demarteau, and A. Roelofs, ACS Nano **8**, 11730 (2014).
[17] L. Li, Y. Yu, G. J. Ye, Q. Ge, X. Ou, H. Wu, D. Feng, X. H. Chen, and Y. Zhang, Nat. Nanotechnol. **9**, 372 (2014).
[18] F. Xia, H. Wang, and Y. Jia, Nat. Commun. **5**, 4458 (2014).
[19] M. A. Ruderman and C. Kittel, Phys. Rev. **96**, 99 (1954).

[20] T. Kasuya, Prog. Theor. Phys. **16**, 58 (1956).
[21] K. Yosida, Phys. Rev. **106**, 893 (1957).
[22] P. J. T. Eggenkamp, H. J. M. Swagten, T. Story, V. I. Litvinov, C. H. W. Swüste, and W. J. M. de Jonge, Phys. Rev. B **51**, 15250 (1995).
[23] F.-s. Liu, W. A. Roshen, and J. Ruvalds, Phys. Rev. B **36**, 492 (1987).
[24] P. D. Gorman, J. M. Duffy, M. S. Ferreira, and S. R. Power, Phys. Rev. B **88**, 085405 (2013).
[25] L. Brey, H. A. Fertig, and S. Das Sarma, Phys. Rev. Lett. **99**, 116802 (2007).
[26] M. A. H. Vozmediano, M. P. López-Sancho, T. Stauber, and F. Guinea, Phys. Rev. B **72**, 155121 (2005).
[27] E. Kogan, Phys. Rev. B **84**, 115119 (2011).
[28] J. J. Palacios, J. Fernández-Rossier, and L. Brey, Phys. Rev. B **77**, 195428 (2008).
[29] A. M. Black-Schaffer, Phys. Rev. B **81**, 205416 (2010).
[30] M. Sherafati and S. Satpathy, Phys. Rev. B **83**, 165425 (2011).
[31] M. Sherafati and S. Satpathy, Phys. Rev. B **84**, 125416 (2011).
[32] F. Parhizgar, M. Sherafati, R. Asgari, and S. Satpathy, Phys. Rev. B **87**, 165429 (2013).
[33] E. H. Hwang and S. Das Sarma, Phys. Rev. Lett. **101**, 156802 (2008).
[34] J. Klinovaja and D. Loss, Phys. Rev. B **87**, 045422 (2013).
[35] P. D. Gorman, J. M. Duffy, S. R. Power, and M. S. Ferreira, Phys. Rev. B **92**, 035411 (2015).
[36] X. Xiao, Y. Liu, and W. Wen, J. Phys.: Condens: Matter **26**, 266001 (2014).
[37] M. Zare, F. Parhizgar, and R. Asgari, Phys. Rev. B **94**, 045443 (2016).
[38] J.-J. Zhu, D.-X. Yao, S.-C. Zhang, and K. Chang, Phys. Rev. Lett. **106**, 097201 (2011).
[39] M. Shiranzaei, H. Cheraghchi, and F. Parhizgar, Phys. Rev. B **96**, 024413 (2017).
[40] A. A. Khajetoorians, J. Wiebe, B. Chilian, S. Lounis, S. Blügel, and R. Wiesendanger, Nat. Phys. **8**, 497 (2012).
[41] L. Zhou, J. Wiebe, S. Lounis, E. Vedmedenko, F. Meier, S. Blügel, P. H. Dederichs, and R. Wiesendanger, Nat. Phys. **6**, 187 (2010).
[42] A. T. Hindmarch and B. J. Hickey, Phys. Rev. Lett. **91**, 116601 (2003).
[43] P. Stano, J. Klinovaja, A. Yacoby, and D. Loss, Phys. Rev. B **88**, 045441 (2013).
[44] H. Duan, S. Li, S.-H. Zheng, Z. Sun, M. Yang, and R.-Q. Wang, New J. Phys. **19**, 103010 (2017).
[45] M. Zare, F. Parhizgar, and R. Asgari, J. Magn. Magn. Mater. **456**, 307 (2018).
[46] G. Yang, S. Xu, W. Zhang, T. Ma, and C. Wu, Phys. Rev. B **94**, 075106 (2016).
[47] E. Taghizadeh Sisakht, F. Fazileh, M. H. Zare, M. Zarenia, and F. M. Peeters, Phys. Rev. B **94**, 085417 (2016).
[48] J. Qiao, X. Kong, Z.-X. Hu, F. Yang, and W. Ji, Nat. Commun. **5**, 4475 (2014).
[49] A. N. Rudenko and M. I. Katsnelson, Phys. Rev. B **89**, 201408(R) (2014).
[50] Y. Zhang, T.-T. Tang, C. Girit, Z. Hao, M. C. Martin, A. Zettl, M. F. Crommie, Y. R. Shen, and F. Wang, Nature **459**, 820 (2009).
[51] W. A. Harrison, *Elementary Electronic Structure: Revised* (World Scientific, River Edge, N.J., 2004).
[52] P. Dutta, S. K. Maiti, and S. Karmakar, J. Appl. Phys. **114**, 034306 (2013).